Real-Time Neural Network-Based Gait Phase Estimation Using a Robotic Hip Exoskeleton

Inseung Kang , *Student Member, IEEE*, Pratik Kunapuli, and Aaron J. Young

Abstract—Lower limb exoskeletons provide assistance during the gait cycle using a state variable, one in particular is gait phase. This is crucial for the exoskeleton controller to provide the user accurate assistance. Conventional methods often utilize an event marker to estimate gait phase by computing the average stride time. However, this strategy has limitations in adapting to dynamic speeds. We developed a sensor fusion-based neural network model to estimate the gait phase in real-time that can adapt to dynamic speeds ranging from 0.6 to 1.1 m/s. Ten able-bodied subjects walked with an exoskeleton using our estimator and were provided with corresponding torque assistance. Our best performing model had RMSE below 29 ms and 4% for real-time estimation and torque generation, respectively, reducing the estimation error by 36.0% ($p < 0.01$) and torque error by 40.9% ($p < 0.001$) compared to conventional methods. Our results indicate that creating a general user-independent model and additionally training on user-specific data outperforms the user-specific model and user-independent model. Our study validates the feasibility of using a sensor fusion-based machine learning model to accurately estimate the user's gait phase and improve the controllability of a lower limb exoskeleton.

Index Terms—Exoskeleton, gait phase estimation, machine learning, sensor fusion, neural network.

I. INTRODUCTION

RECENT technological advancement in the field of lower-limb exoskeletons has opened numerous opportunities in the domain of human augmentation [1], [2]. The applications of these exoskeletons can be expanded to several areas such as human performance enhancement, wearable robotics for daily assistance, and rehabilitation in healthcare settings [3]–[5]. The advantage of using powered exoskeletons comes from their ability to implement different controllers to provide assistance during locomotion [6]–[13]. These exoskeleton controllers heavily rely on understanding the user's state, such as gait phase, during locomotion so that the device can correctly assist at the desired timing. Gait phase, a continuous variable representing the gait cycle, is defined as a linearly increasing value between 0 and 100, where both values represent heel contact on a single leg during locomotion. Accurate estimation of the gait phase is paramount for the device to provide assistance at the desired timing to the user, resulting in optimal performance [14], [15].

Different strategies have been introduced to estimate user gait phase. A common method is to estimate the gait phase using a mechanical sensor such as a force sensitive resistor (FSR) sensor placed at the heel [16], [17]. From the FSR sensor, average stride time can be computed from some previous number of steps and the user's gait phase is determined from the time since last heel contact compared to the average stride time. While this method is easy to implement, it has many drawbacks including the need to place the sensor in a distal area and the inability of the method to adjust to speed changes quickly, since many steps need to be taken for the average stride time to converge to another value. Another method is to use a finite state machine and segment the gait phase into discrete events (i.e., stance and swing phase). Different mechanical sensors are used to trigger transitions through the state machine, and each state has unique assistance [18]–[20]. The drawback of this approach is since states are represented discretely as opposed to continuously, transitions may not be seamless and multiple assistance controllers must be developed, one for each state. Another method used in the literature is incorporating a phase variable approach with the hip joint angle [21], [22]. This method leverages the sinusoidal nature of hip joint angle during level walking and converts the joint angle into gait phase. This phase variable approach is more robust compared to the FSR-based method since it maps the hip joint configuration into gait phase directly making it more accurate than a moving average. However, this method still requires the user to be in a rhythmic motion (i.e., constant walking) and cannot accommodate abrupt changes in walking speeds such as stopping. Lastly, other research groups applied a more complex method of using an adaptive oscillator approach [23], [24]. This method also employed the idea of the hip joint trajectory being a sinusoidal wave. The algorithm understands the frequency and the envelope from the user's joint trajectory and generates a similar sine wave representing the user's gait phase. This method is a robust method of adapting to different walking speeds. However, if a user experiences a sudden change to their walking pattern (i.e., stumble), the estimation can become unsynchronized. Furthermore, this method is far more complex than the other two methods, which

requires subject-specific tuning and may increase the overall computational cost when implementing it to an autonomous device.

One possible solution to such problems involves machine learning (ML). Some research groups have started to utilize different ML techniques using a mechanical sensor from the device to understand the user's gait dynamics [25], [26]. In order to further improve the model's robustness, ML with sensor fusion techniques can be applied [27], [28]. By utilizing a multi sensor modality through a sensor fusion approach, different mechanical sensors on the exoskeleton device can add meaningful information to comprehend the user's gait phase more accurately. This approach will also allow the device to accommodate the user's dynamic movement more accurately. Although there are a plethora of ML models being developed and researched, neural networks have gained recent attention for their use in deep learning tasks [29], and the power of neural networks to learn difficult and complicated tasks is well documented [30]. Additionally, once trained, neural networks are amenable to real-time processes on an embedded system via implementation as a series of matrix operations. Thus, we elected to follow deep learning approaches in adopting a neural network for our machine learning task.

The main purpose of this study was to test the hypothesis that the multi sensor fusion-based machine learning model performs with higher accuracy in estimating the user's gait phase than the event detection method using a mechanical sensor during dynamic speed locomotion tasks. Our sub-hypothesis is that a model trained with user-specific data will have less estimation error, especially in dynamic settings, compared to a generalized model [31]. To test our hypothesis, we used a powered bilateral hip exoskeleton incorporated with different gait phase estimator methods. Our estimator utilized a neural network machine learning model to estimate user gait phase from the hip joint angle and thigh IMU data. The overall goal of our study was to better understand the feasibility of implementing the machine learning model to estimate the user's state in a real-time application. This accurate high-level estimation of human locomotion using a sensor fusion strategy will help exoskeleton and other wearable robotics developers to improve device performance.

II. INITIAL SYSTEM CHARACTERIZATION

A. Powered Hip Exoskeleton

Our study utilized a previously designed powered bilateral hip exoskeleton (Fig. 1A) [32]. The device comprises two ball screw driven series elastic actuators (SEAs) using brushless DC motors (EC30, Maxon Motors, Switzerland) with an initial timing belt gear reduction. The actuator output linkage incorporates a fiberglass spring with a strain gauge, allowing a closed loop low-level torque control. The exoskeleton houses several on-board mechanical sensors (Fig. 1B). The device has two 14-bit absolute magnetic encoders (Orbis, Renishaw, U.K.) placed at the actuator output that measure the hip joint angles bilaterally. Three inertial measurement units (Micro USB, Yost Lab, USA) (IMUs) are mounted on the device: two located on each thigh segment bilaterally and one on the trunk
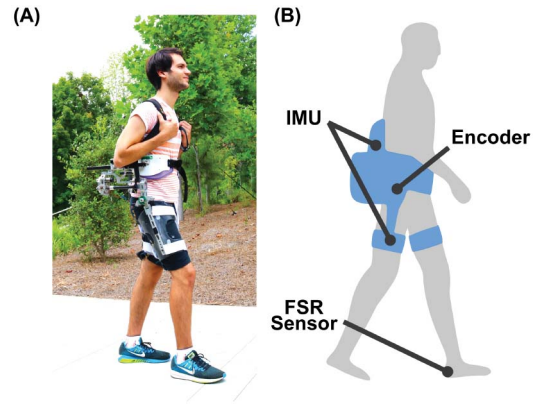

Fig. 1. Powered bilateral hip exoskeleton. (A) The device can provide power assistance along the sagittal plane. The user interface can be adjusted to accommodate different user body sizes. (B) Multiple mechanical sensors are placed on the device to measure the user's movement. The IMUs are placed one on the trunk and one on each thigh segment, encoders are located at the hip joint bilaterally, and the FSR sensors are placed at each heel of the user.

to measure the limb orientations. The IMUs instrumented on the device can compute the Euler angles through a built-in Kalman filter, representing their orientation in three dimensions. Lastly, FSR sensors are placed on each heel to detect the heel strike during walking. All the sensors and actuators were commanded using a microprocessor incorporated with an FPGA (myRIO, National Instruments, USA). All the on-board sensor data was sampled and recorded at 100 Hz.

The overall control architecture of our device is broken down into high-, mid-, and low-level layers. The high-level layer incorporates different types of gait phase detection algorithms and estimates the gait phase in real-time. The gait phase is then passed down to the mid-level layer, where the control loop generates a desired torque assistance profile. For this study, the mid-level controller had two different implementations. For the initial data collection experiment, we used a "zero impedance" mode, which refers to the actuator cancelling out any interaction torque measured (by commanding 0 Nm torque) at the hip joint so that the user feels natural in movement. For the real-time experiment with active torque generation, we used a controller that mimics the nature of biological hip moment profile shape [33]. The desired torque profile was generated in a form of a sinusoidal wave with predefined peak torque magnitude occurring at 0% (heel strike) of the gait cycle for hip extension and 50% of the gait cycle for hip flexion. Lastly, a low-level layer receives the commanded torque and ensures that the correct torque is being provided to the user through a closed loop PID torque controller utilizing the SEA design.

B. Data Collection for Model Optimization

The study was approved by the Georgia Institute of Technology Institutional Review Board, and informed written consent was obtained for all subjects. Eight healthy subjects with an average age of 22.3 ± 2.4 years, height of 1.77 ± 0.06 m, and body mass of 74.4 ± 7.6 kg were asked to walk on the treadmill (TuffTread, USA) with the powered hip exoskeleton for 2 minutes at walking speeds ranging
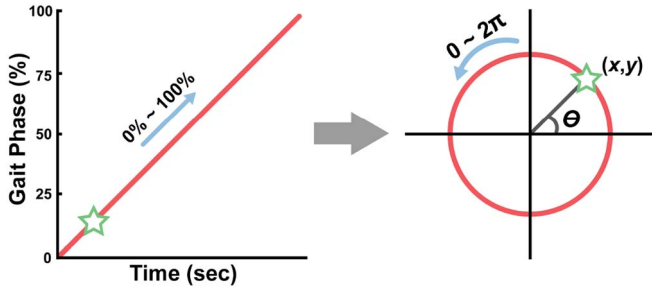
Fig. 2. Gait phase output conversion. To eliminate the inherent discontinuity of a gait phase output (where 100% is equal to 0%), the signal is converted to a unit polar coordinate system where the gait phase is represented as (x, y). An example of gait phase conversion is shown with a green star.
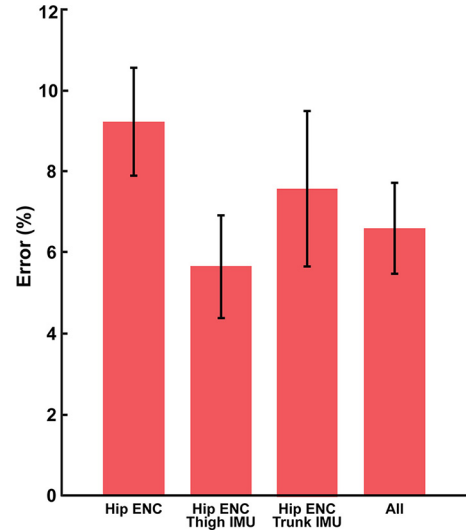

Fig. 3. Sensor selection error results. Machine learning model error was measured in the same model with various sensor combinations to find the minimum number of sensors with lowest error. Error bars in the graph represent the 95% confidence interval.

from 0.6 m/s to 1.0 m/s with an increment of 0.05 m/s for a total of 18 minutes. The exoskeleton was put into zero impedance mode for all 9 conditions. During all walking conditions, mechanical sensor data from the right thigh and trunk IMUs, the hip joint angle from the encoder, and the heel contact information (for ground truth calculation) from the FSR sensor were recorded. All eight subjects' data was used for training the baseline neural network model.

C. Neural Network Model Offline Optimization

Raw FSR sensor voltages were used for the ground truth calculation of a user's gait phase percentage. Each rising edge of the signal acted as an event marker representing the heel strike, and the gait phase percentage was linearly interpolated between heel strikes as 0% to 100%, wrapping back to 0% at the next heel strike. However, this results in discontinuities in the gait phase percentage, as the signal would go from 99% to 0% suddenly.

In order to avoid modeling the discontinuity in the machine learner, we transformed the gait phase percentage into a polar coordinate (Fig. 2), where the angle, θ, represented the gait phase percentage between 0 and 2π (Equation 1). Using Equations 2 and 3, we then represented the gait phase as 2 variables, x and y, where at the boundary condition of a heel strike there is no longer a discontinuity in the Cartesian outputs. Without this transformation, computing the error of the machine learning estimation would have a bias at heel contact, since the error between just before and just after heel contact would be computed as 100% without the polar conversion. By using the polar conversion, we can compute the error between estimation and ground truth as the angle between the two vectors in the polar representation, removing the bias at heel contact.

$$\theta = \frac{gait\ phase\ percentage}{100} \cdot 2\pi \quad (1)$$
$$x = cos(\theta) \quad (2)$$
$$y = sin(\theta) \quad (3)$$

A baseline fully connected neural network with one layer and 20 neurons was used to evaluate the feature-dependent hyperparameters such as sliding window size and which features were relevant. Following previous methods of feature extraction for mechanical sensors such as IMUs and

encoders [34], six features were computed for each sensor signal: min value, max value, mean, standard deviation, first value and last value. The sensor signals collected were the hip encoder angle, three Euler angles from the thigh IMU and three Euler angles from the trunk IMU, and the six features were computed for all seven of these signals resulting in a total of 42 features. The sliding window size was swept through, and the size that yielded the highest accuracy was 300 ms in this baseline neural network. First, the sliding window size was swept through to find the window size that yielded the highest accuracy (300 ms). Next, both sequential forward feature selection for all 42 features and sequential forward sensor selection for the seven sensors (groups of six features) was done with the baseline neural network model to evaluate which features were the most relevant. During sequential forward feature selection, every permutation of the 1 to 42 features was tested to determine the individual feature contributions in reducing the overall error. During sensor selection, each permutation of 1 to 7 sensors was tested. We performed leave-one-user-out validation to avoid user-based bias. Since we were limited by the amount of data to collect, we needed to simplify the machine learning problem by eliminating features that are less relevant to gait phase estimation via feature or sensor selection in order to avoid the "curse of dimensionality" [35].

Sensor selection yielded machine learning model errors of $9.20 \pm 1.92\%$ with the hip encoder only, $5.65 \pm 1.83\%$ with the hip encoder and thigh IMU, $7.56 \pm 2.77\%$ with the hip encoder and trunk IMU, and $6.55 \pm 1.62\%$ with all sensors. This sensor selection demonstrated that the hip encoder and the thigh IMU were the most important sensors (Fig. 3). One possible explanation for the reduced accuracy when using all sensors is the limitation of the static baseline neural network model used to evaluate the features. It is possible that a more complex model is needed to estimate gait phase from all sensors and could result in higher overall accuracy, but to test

all sensor combinations fairly the same neural network model was used. The sequential forward feature selection confirmed the results from the sensor selections and additionally, showed that the Z-axis (transverse plane) Euler angles were much less favored compared to the X-axis (sagittal plane) or the Y-axis (frontal plane) Euler angles.

After finalizing the dataset with the features and ground truth, three different fully connected neural network models were created to optimize the estimation task from the data. In the "independent model" (IND), a model is trained on all but one subject and then tested on the subject that was withheld. This model represents a generalized model applied to a new user, leveraging a large amount of data from a collection of other users [31]. In contrast, the "dependent model" (DEP) was trained on a subset of a single user's data, and then tested on the rest of that user's data not yet seen by the model. This model represents a user-specific model aimed at optimizing the accuracy as much as possible by solely learning a single user's gait patterns. Finally, the "semi-dependent model" (SEMI) was a mixture of the two aforementioned methods, where the model starts from a pre-trained IND and then additionally trains on a small subset (half) of a single user's data with higher weighting and tested on the rest of that single user's data. Following a transfer learning approach, this SEMI aims to maximize the accuracy for a single tested user while minimizing the data needed from that user since it can leverage data from other users. All of the neural networks were trained in Python using Keras [36] with a TensorFlow GPU [37] backend. The models were trained on a computer with an AMD 2700X CPU (AMD, USA) and two Nvidia GTX 1070 GPUs (ASUS, Taiwan).

In order to maximize estimation accuracy for the three different models, the neural network parameters were swept through to find the highest estimation accuracy. All parameters were tuned following standard literature methods with a common dataset from all subjects (user-independent model) [38]. The model parameters were kept the same between all three models to evaluate them fairly against each other. Additionally, since they were later implemented in real-time, the models needed to be of the same size for the same computation cost on the device. The size of the input and output layers of the network are fixed from the application paradigm (17 features and 2 outputs, respectively). Some of the hyper-parameters that were swept were the network architecture for both the number of layers (1-3) as well as number of nodes per layer (10-30, in increments of 5), batch size in the set {16, 32, 64, 128, 256}, optimizer in the set {stochastic gradient descent (SGD) with Nesterov momentum [39], [40], ADAM, RMSProp, AMSGrad}, learning rate in the set {0.1, 0.25, 0.5, 1, 2, 5, 10}, and activation functions for the hidden layers in the set {tanh, ReLU, sigmoid, linear}. Although larger and more complex network architectures would in theory perform better, we were limited by the computation capability in the real-time implementation of machine learning algorithm on the hip exoskeleton device. The final hyper-parameters selected that minimized estimation error were 20 neurons in the single hidden layer, SGD optimizer with Nesterov momentum, a learning rate of 0.001, tanh activation function for the hidden
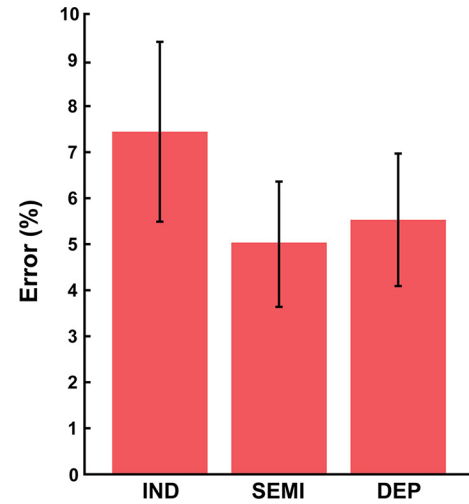

Fig. 4. Offline comparison of gait phase estimator error across different user models. With optimal neural network hyper-parameters, resulting model had an error of $7.44 \pm 2.82\%$, $5.04 \pm 1.96\%$, and $5.53 \pm 2.08\%$ for the IND, SEMI, and DEP respectively. Error bars in the graph represent the 95% confidence interval.

layer, linear activation function for the output layer, and a batch size of 128. All models were trained with the mean absolute error (MAE) as a loss function. For the SEMI model, there is one unique parameter that does not exist for the other models, the relative importance of the specific user data compared to the other subjects, and it was swept through in the set {5, 10, 20, 30, 40, 50, 60, 70, 80, 90, 100}, resulting in a weighing of 80:1 which maximized the accuracy. In order to prevent overfitting, all models were trained for a maximum of 200 epochs, stopping early if the validation loss did not continue to decrease in 5 epochs [41]. Additionally, training was done with 10-fold cross validation as well as leave-one-subject-out validation to remove bias across users. After the neural network parameters were optimized, the feature optimization was performed again on the optimized neural network model rather than the baseline neural network model to ensure the features chosen were still the best, and the results were the same. The final offline results showed that the SEMI performed the best (Fig. 4).

III. METHODS

A. Experimental Protocol

The study was approved by the Georgia Institute of Technology Institutional Review Board, and informed written consent was obtained for all subjects. For experimental validation of the gait phase estimator, ten healthy subjects (different from the original eight healthy subjects for initial data collection) with an average age of 21.3 ± 1.8 years, height of 1.79 ± 0.06 m, and body mass of 75.1 ± 4.9 kg were initially asked to walk on a treadmill for 5 minutes with a powered hip exoskeleton and treadmill speed ranging from 0.6 m/s to 1.0 m/s using a predefined speed profile, thus emulating the pilot experiment (Fig. 5A). During the initial walking trial, the hip exoskeleton was controlled in a zero impedance mode, and the relevant sensor data from the pilot experiment (the hip encoder and thigh IMU) were collected, as well as the FSR sensor for ground truth labeling only. Using the data collected
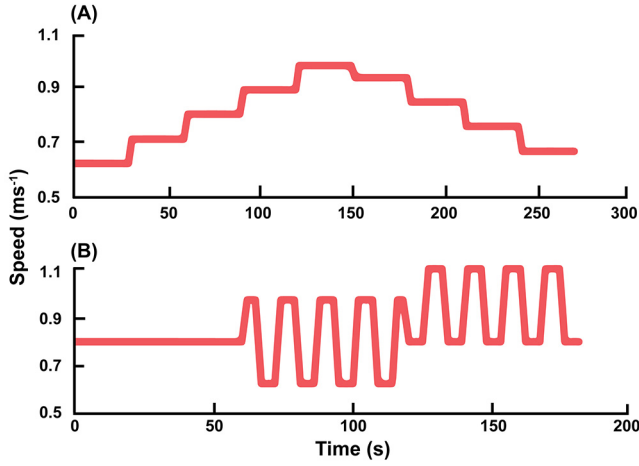
Fig. 5. Treadmill speed profile for experimental validation of the gait phase estimator. (A) Speed profile emulating the pilot experiment. The data were collected to generate the user dependent and semi-dependent model. (B) Speed profile for testing the gait phase estimator. The profile was set to evaluate model accuracy in dynamic speed range settings.

during the training trial, the DEP and SEMI were generated on a separate computer. After all the models were trained, subjects walked for 3 minutes on the treadmill with a powered hip exoskeleton for each condition where the first minute had a constant walking speed of 0.8 m/s, the second minute had a predefined speed profile ranging from 0.6 m/s to 1.0 m/s, and the third minute had a predefined speed profile ranging from 0.8 m/s to 1.1 m/s (Fig. 5B). The maximum walking speed was defined based on the capabilities of the exoskeleton, as this was the highest walking speed at which the device could track torque accurately. While the operating speed did not capture all the walking speed ranges (i.e., 1.5 m/s), we believe that similar results can be expected in higher walking speed ranges as the kinematic information at faster walking speed does not vary too much from our tested walking speed ranges [33].

The testing speed profile was chosen to represent and validate three parts: a model performance in constant walking speed, in speed range within the training data, and in speed range outside of the training data (to observe model's capability in extrapolation). During walking, four different gait phase estimator methods were implemented: time-based estimation (TBE) using FSR sensor from the previous five strides (literature standard for baseline comparison), and the same estimators developed from the pilot experiment (IND, DEP, and SEMI). While previous literature study used 10 strides for the TBE method, this may greatly either lead or lag the overall system when there is a speed change. On the other hand, using smaller number of strides (2 or 3 strides) can induce higher estimation errors during steady state walking due to the user's gait variation on a stride-by-stride basis. From a pilot testing and our previous study using the same TBE method on our hip exoskeleton [15], we found that using 5 strides for the average stride duration was optimal.

For all walking conditions, the tested gait phase estimator generated a sinusoidal torque command with a peak torque magnitude set to 1 Nm. Because the testing speed profile

examines three aspects of the estimator performance, the results were segmented into three parts. Part A corresponds to the first section in the trial representing the steady state walking speed. Part B corresponds to the second section representing the dynamic movement where the walking speed is changing in the same range that the machine learning models were trained. Lastly, Part C corresponds to the dynamic movement where the walking speed is changing in a range not entirely within the range that the machine learning models were trained.

B. Real-Time Machine Learning Model Implementation

Following the outcome of the pilot experiment, the real-time implementation of the three machine learning models was thoroughly validated. First, the feature selection process was verified between the offline calculation in Python and the real-time implementation on the myRIO microprocessor inside the hip exoskeleton. Machine learning models were implemented on the device after verifying the proper computation of the features in a rolling window of 300 ms updating every 10 ms. The overall matrix computation of the neural network model can be represented as Equation 4, where F is the feature vector of size 17×1, H is the hidden layer vector of size 20×1, and G is the output vector of size 2×1. W_i represents the weight matrix at layer i, and B_i represents the bias vector at layer i.

$$H = tanh(W_1 F + B_1)$$
$$G \triangleq \begin{bmatrix} x \\ y \end{bmatrix} = W_2 H + B_2 \qquad (4)$$

The output of the neural network model is the pair (x, y) in polar coordinates, which corresponds to the gait phase via Equations (2) and (3). In order to convert back to a percentage, which is needed for the sinusoidal torque profile calculation on the exoskeleton, Equation (5) is used.

$$gait\ percent = \left(\left(tan^{-1}\left(\frac{y}{x}\right) + 2\pi \right) mod : 2\pi \right) \times \frac{100}{2\pi} \quad (5)$$

C. Torque Profile Generation

Lastly, using the real-time gait phase estimation, the torque profile applied to the user is generated in real-time using Equation (6) (Fig. 6).

$$\begin{cases} \tau_{right} = cos\left(gait\ phase\ percent \times \frac{2\pi}{100} \right) \\ \tau_{left} = -cos\left(gait\ phase\ percent \times \frac{2\pi}{100} \right) \end{cases} \quad (6)$$

A sinusoidal torque is commanded to both sides of the device. The peak torque of 1 Nm (extension) appears at 0% and 1 Nm (flexion) at 50% of the gait cycle for each leg to represent the hip extension and flexion assistance. 1 Nm peak torque is chosen to demonstrate the actual effects of the high level gait phase algorithm on control performance, but without errors adversely affecting the user.

D. Statistical Analysis

The FSR sensor was used to calculate the ground truth gait phase percentage, and the corresponding ground truth torque profile was generated by applying Equation 6. All results were
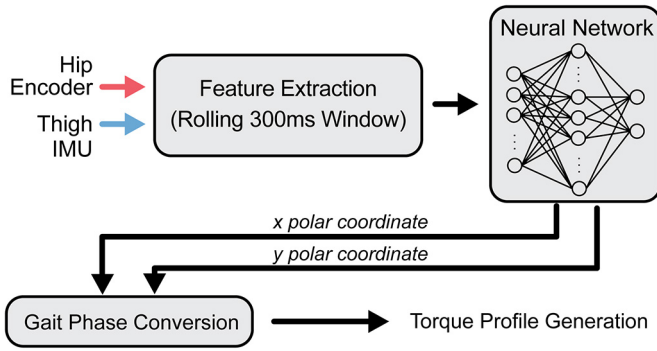
Fig. 6. Overall flow chart of the gait phase estimator performance validation. Feature extraction, matrix computation, and torque profile generation occurs sequentially to provide hip assistance to the user bilaterally in real-time.

computed by comparing the gait phase estimation and torque applied to the ground truths and calculating the root mean squared error (RMSE). We conducted a repeated measures one-way ANOVA test to compare the estimator performance across the three parts, and a Bonferroni *post-hoc* correction ($\alpha = 0.05$) for a pairwise comparison across multiple measures.

IV. Results

Overall, all machine learning methods were able to perform well in the real-time implementation. Generally, machine learning strategies performed better during dynamic (changing speed) conditions. An example of real-time exoskeleton performance of estimating the gait phase over 8 steps of the user semi-dependent (the best performing ML algorithm), and time-based estimation (TBE) relative to the ground truth is shown in Fig. 7.

A. Real-Time Gait Phase Estimator Performance

In the steady state portion (Fig 8A), none of the strategies performed significantly differently for gait phase estimator RMSE or torque RMSE. However, in the dynamic conditions (Fig. 8B+C), both the SEMI and DEP machine learning strategies significantly ($p < 0.05$) outperformed the TBE method. Additionally, in the high speed range (Fig. 8C), the SEMI model performed significantly better than the IND model ($p < 0.05$). These statistical trends were consistent between both the RMSE of the gait phase estimator and the torque generation. In summary for torque generation during dynamic movements (Parts B and C), the IND reduced average torque generation error by 18.9% ($p = 0.55$), SEMI by 40.9% ($p < 0.05$), and DEP by 32.4% ($p < 0.05$) compared to the TBE strategy. We further investigated these trials to quantify the estimation accuracy by differentiating the dynamic trials into steady-state and dynamic sections. The average RMSE for the steady-state section were $4.83 \pm 0.62\%$ and $5.07 \pm 0.49\%$ while the dynamic section average RMSE were $8.11 \pm 2.19\%$ and $5.22 \pm 0.81\%$ for the TBE and SEMI, respectively across all subjects.

B. Training Time of Semi-Dependent and Dependent Models

The SEMI and the DEP were both trained on the user-specific data from the training trials. The SEMI converged for a much lower number of epochs, representing the number of times observing the training set compared to the DEP. On average across subjects, the SEMI converged after 43.80 ± 5.28 epochs. The DEP converged on average after 174.60 ± 12.71 epochs.

V. Discussion

The primary contribution of this study was to develop and evaluate a sensor fusion-based machine learning model for estimating user gait phase in real-time using a powered hip exoskeleton. The SEMI and DEP models on average performed better than the baseline time-based estimation (TBE) by reducing the estimation error rate by 26.3% and 23.4% respectively across all three walking conditions. The IND performed similarly to the TBE by having a slight increase in the estimation error rate by 0.7%. Specifically, during the dynamic trials, the machine learning models outperformed the TBE (as shown in Fig. 7) where the TBE either led or lagged in estimation when the user was changing speeds as indicated by the increased RMSE (by 5 times) compared to the steady-state section. These results clearly illustrate the power of machine learning having superiority over the TBE when the user is dynamically accelerating or decelerating. This corresponds to our original hypothesis that the neural network-based model can adapt to different walking speeds because of the prior gait phase pattern that the model has seen from the training dataset. The significance of our models handling the dynamic tasks is that these tasks resemble closely to what people would experience in the real-world where there is a lot of start/stop and changing speeds. A possible implication of having an accurate gait phase estimator is reducing the user's metabolic cost which has been considered as a "gold standard" outcome measure in the field of exoskeleton. Different literature studies have shown that assistance timing (which is directly related to the user's gait phase) is a critical control parameter for maximizing the energetic benefit [7], [8], [14], [17], [42], [43]. Previous assistance timing studies in the literature indicated that approximately 10% change in the assistance onset or peak timing can correlate up to on average of 2.5% in metabolic cost difference [8], [14], [17], [43]. These results illustrate that the implementation of a robust gait phase estimator is critical for maximizing the overall human exoskeleton performance from an energetics perspective.

The key difference within the machine learning models was the amount of user-specific data allowed. The IND is the most convenient model out of the three models as it requires no new data from the user. However, the IND does not perform better than the TBE during the steady state speed and only slightly better during the dynamic tasks. On the other hand, the SEMI and DEP models are trained on and able to learn the user-specific gait pattern to significantly outperform the TBE during the dynamic tasks including the extrapolated speed ranges. Overall, the SEMI performed the best among the machine learning models because it aims to maximize the accuracy for a given subject while utilizing the general dataset which contains different gait pattern variations across other subjects. Although the DEP, in theory, should have performed the best
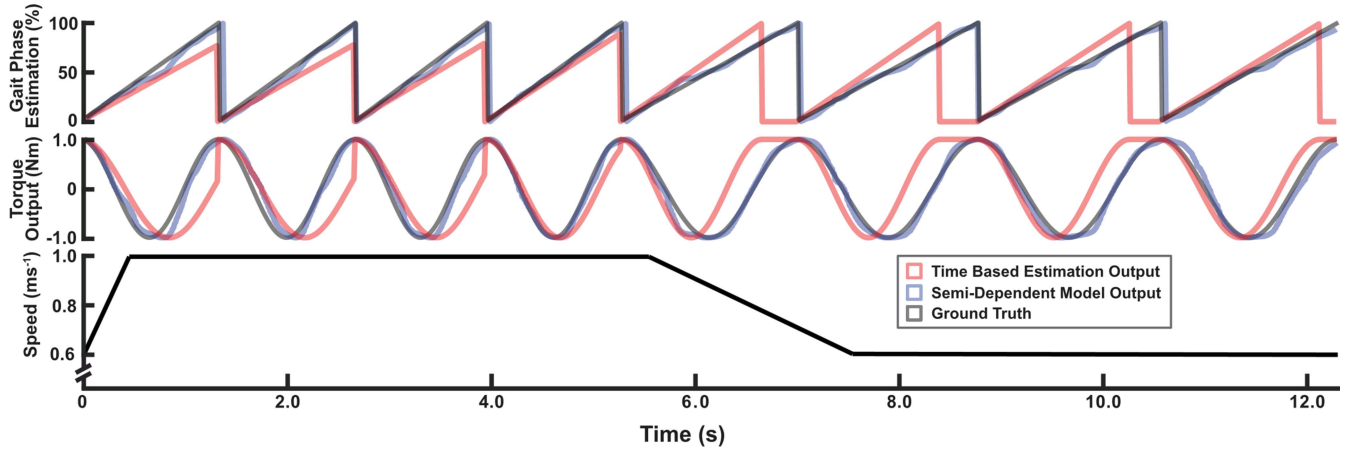
Fig. 7. Real-time performance of both the TBE and the SEMI against the ground truth over 8 strides with the corresponding walking speed. When the walking speed either accelerates (0s ∼ 0.5 s) or decelerates (5.5 s ∼ 7.5 s), the TBE (using previous 5 strides as the average stride duration) takes several additional steps to update the gait phase estimation while the SEMI is capable of adapting to dynamic speed changes instantaneously. Due to poor estimation during dynamic speed ranges, corresponding torque profile generated from the TBE has discontinuity while the SEMI does not.
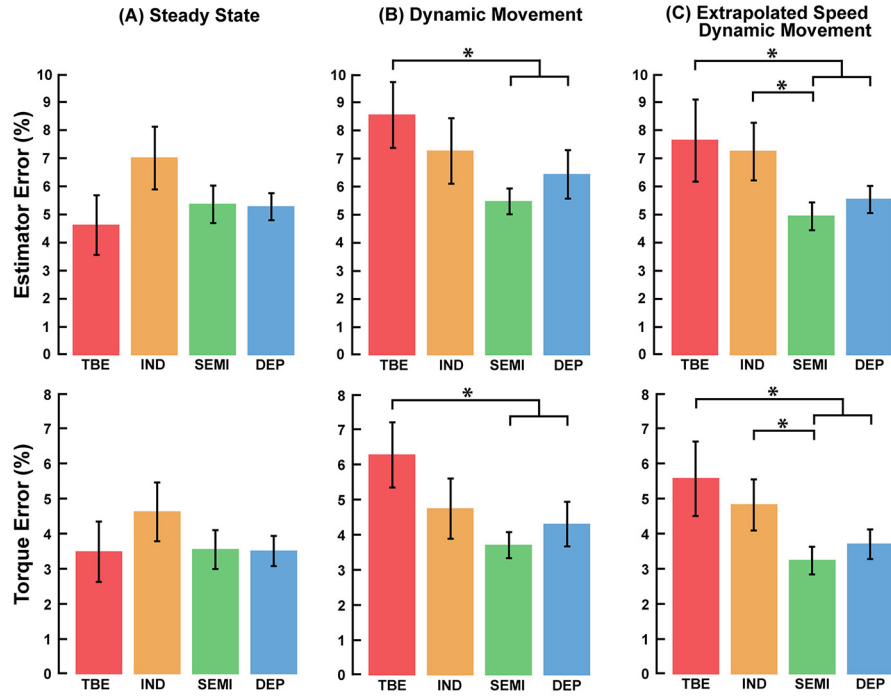

Fig. 8. Real-time gait phase estimation results. The speed trial had three parts to comprehend dynamic speed changes to evaluate the estimator performance. (A) Overall performances were similar during steady state walking speed where the TBE performed the best. (B) During the dynamic speed changes within the speed range of training dataset, the SEMI performed the best. (C) Similar trends to (B) were shown for the dynamic speed changes with speed range outside of the training dataset where all user models were able to extrapolate and estimate the gait phase correctly and the SEMI performed the best. Asterisks indicate the estimator that had significantly lower error between two conditions in the pairwise Bonferroni *post-hoc* test. Data were averaged across ten subjects and the error bars in the graph represent the 95% confidence interval.

amongst the three machine learning-based models in real-time, the SEMI performed slightly better. This is most likely due to the fact that the SEMI model leverages the pre-trained IND as well as subject-specific data, which is overall more data compared to the DEP [44]. Furthermore, the SEMI trains for a much smaller number of epochs than the DEP, which represents the fact that less user-specific data is needed to learn by leveraging the IND to train from. However, in the case where obtaining a pool of training data is not easily available (i.e.,

patient population), the DEP may be the only feasible solution for gait phase estimation.

Since the real-time torque applied from the hip exoskeleton was directly mapped from the estimated user gait phase, it is evident that the gait phase estimator accuracy dictates the overall exoskeleton controllability. A linear correlation between the average RMSE for the estimators in all three walking conditions and the corresponding average torque generator RMSE yielded an adjusted R^2 value of 0.941 ($p <$

0.01), demonstrating a strong positive correlation between the errors in these two areas. Depending on the types of controller chosen, the torque generator RMSE may be different but the correlation between estimator performance and torque performance is directly related. During our experiment, we chose a mid-level controller (sinusoidal wave) that would mitigate the gait phase estimation errors from the TBE, especially at the heel contact (0 or 100%), in order to ensure a smooth torque output to the user. Because of this, the TBE had a slight advantage compared to other estimators when comparing the torque error, since errors around heel contact were mitigated by the sinusoidal nature of the torque controller chosen. However, this would not be the case if another mid-level control paradigm is used instead. Although the amount of torque applied was lower than other studies, the primary finding that a machine learning-based gait phase estimator can assist the mid-level torque generation across different speeds holds.

Our machine learning models outperformed different methods that have been used in previous literature. The baseline method TBE, adopted by several groups for their exoskeletons due to its simplicity, did not yield robust estimation results during the dynamic tasks as predicted [16], [17], [45]. Moreover, even during a steady state walking, the TBE did not show any significant benefits (approximately 2.5% error difference compared to the worst performing IND). Considering its performance, our results indicate that the TBE is appropriate for experiments with a fixed treadmill speed but is not appropriate for dynamic speed tasks. Other groups have implemented more advanced methods for estimating gait phase such as phase variables or adaptive oscillators which can be more adaptable and continuously estimate the gait phase [46]–[48]. One example is using hip angles as a phase variable to estimate the gait phase [21], [22]. Based on our analysis, this method has substantially more phase estimation error than the sensor fusion-based approach during dynamic speed changes. Phase variable approach often requires couple of strides for the model to update to a new steady-state walking speed where as our comparable IND model only takes 29 ms to adapt in similar walking speed ranges. Some limitations for the adaptive oscillator approach are the detailed subject-specific tuning and a higher computational burden when considering real-time implementation on a microprocessor. Compared to our DEP model, the adaptive oscillator method performs with a similar error rate during steady-state or gradual speed changes, but it cannot robustly accommodate to abrupt changes in the user's walking speeds (specifically during acceleration), and has a long delay time when returning to steady-state (approximately 12 seconds when tested under comparable speed changes as our study) which is not suitable for highly dynamic, real-world settings [23], [47]. However, recent literature works in developing a non-user-specific adaptive oscillator show better performance than our comparable IND model by approximately 3% gait phase estimation error rate [49], [50]. However, this method requires additional sensors placed outside the device interface region while our approach only utilizes the on-board sensors (i.e., capacitance sensor cuff placed around the shank) which may be a burden from an exoskeleton designer perspective.

One limitation of our study is that the device training and testing profiles were conducted in controlled speed ranges on the treadmill. While this was mainly done to systematically compare the estimator performance equally, this does not fully capture real-world over ground locomotion that would likely have even higher variability and dynamics than the simulated tasks in this study. Another limitation is that our study did not capture the entire range of walking speeds (i.e., fast walking at 1.5 m/s) mainly due to the device limitations. While our models can easily estimate the user's gait phase within the trained speed ranges and can perform well even in the ranges that are slightly outside of the trained dataset, we do not expect similar performance in the speed range far outside the trained dataset mainly due to ML models not being robust in extrapolation [51], [52]. Additionally, we want to acknowledge that our model architecture will need to be different for speed even greater (i.e., 2.5 m/s) as it would be considered running and the hip dynamics will change completely [53]. However, our models (at least the model trained with speed of 0.6 to 1.0 m/s) can be applicable to different scenarios that are potentially quite valuable for the community. For example, in the case of exoskeleton applications in clinical populations such as stroke, SCI, or MS, this speed range is often the preferred zone for many patients with partial movement disorders which is one of the main applications of hip exoskeletons. In such cases, we think that the developed model approach provide meaningful information.

Lastly, we think that the sine wave-based torque profile is not ideal assistance strategy for the user. A simple sine wave was chosen to approximate the biological torque curve. As the biological hip moment greatly resembles a sinusoidal wave, it was easy to implement for actual application. Since our assistance magnitude was not large, it did not provide any discomfort to the user during assistance mode. We matched the phase of the sinusoid so that the torque would be applied in the direction of movement with peak timings matched to biological peak flexion/extension timings. Unless the gait phase estimator had large error (>25%), the subject would not be fighting against the controller. Previous literature studies have indicated that the assistance control parameters can easily change the overall exoskeleton performance [14], [15], [17], [54], and future studies will focus on a more appropriately tuned low level controller.

Our study results show an exciting promise for the future direction of exoskeleton control. While IND model showed a similar performance as to the TBE, it has a greater advantage of not requiring an additional user specific training data. This advantage benefits the user greatly in a scenario where collecting subject specific data is impossible. The SEMI model showcased the power of transfer learning [55] applied to the human-augmentation robotics domain, where the user-specific data is both highly valued and costly to attain especially for patient populations. For example, in a clinical setting, it might not be feasible to collect much data from the patient due to their limited mobility. In this case, the SEMI model using minimal additional user data may be a viable solution. By having accurate user gait phase information, the exoskeleton controller can be tuned to more smoothly provide assistance to

the user compared to simpler state machines. Both the SEMI and DEP strategies minimized error across all conditions and could potentially be viable options for gait phase estimation for exoskeleton devices.

VI. CONCLUSION

We have successfully implemented the user gait phase estimator using a robotic hip exoskeleton in real-time to smoothly control torque generation. Our results indicated that the sensor fusion-based machine learning models can adapt to different walking speeds robustly which can greatly help to generate a more accurate assistance to the user. Additionally, we found that applying a small portion of user-specific data to a general model can vastly increase the overall estimator performance. Future work will focus on exploring the online strategy to generate a gait phase estimator model that can adapt to the user in real-time.

ACKNOWLEDGMENT

REFERENCES

[1] A. J. Young and D. P. Ferris, "State of the art and future directions for lower limb robotic exoskeletons," *IEEE Trans. Neural Syst. Rehabil. Eng.*, vol. 25, no. 2, pp. 171–182, Feb. 2017.

[2] T. Yan, M. Cempini, C. M. Oddo, and N. Vitiello, "Review of assistive strategies in powered lower-limb orthoses and exoskeletons," *Robot. Auton. Syst.*, vol. 64, pp. 120–136, Feb. 2015.

[3] H. Yu, I. S. Choi, K.-L. Han, J. Y. Choi, G. Chung, and J. Suh, "Development of a upper-limb exoskeleton robot for refractory construction," *Control Eng. Pract.*, vol. 72, pp. 104–113, Mar. 2018.

[4] F. A. Panizzolo *et al.*, "A biologically-inspired multi-joint soft exosuit that can reduce the energy cost of loaded walking," *J. Neuroeng. Rehabil.*, vol. 13, no. 1, p. 43, 2016.

[5] S. A. Kolakowsky-Hayner, J. Crew, S. Moran, and A. Shah, "Safety and feasibility of using the EksoTM bionic exoskeleton to aid ambulation after spinal cord injury," *J. Spine*, vol. 4, no. 3, pp. 1–8, 2013.

[6] L. M. Mooney, E. J. Rouse, and H. M. Herr, "Autonomous exoskeleton reduces metabolic cost of human walking during load carriage," *J. Neuroeng. Rehabil.*, vol. 11, no. 1, p. 80, 2014.

[7] J. Zhang *et al.*, "Human-in-the-loop optimization of exoskeleton assistance during walking," *Science*, vol. 356, no. 6344, pp. 1280–1284, 2017.

[8] S. Galle, P. Malcolm, S. H. Collins, and D. De Clercq, "Reducing the metabolic cost of walking with an ankle exoskeleton: Interaction between actuation timing and power," *J. Neuroeng. Rehabil.*, vol. 14, no. 1, p. 35, 2017.

[9] D. P. Ferris and C. L. Lewis, "Robotic lower limb exoskeletons using proportional myoelectric control," in *Proc. IEEE Annu. Int. Conf. Eng. Med. Biol. Soc.*, 2009, pp. 2119–2124.

[10] K. Seo, J. Lee, Y. Lee, T. Ha, and Y. Shim, "Fully autonomous hip exoskeleton saves metabolic cost of walking," in *Proc. IEEE Int. Conf. Robot. Autom. (ICRA)*, 2016, pp. 4628–4635.

[11] J. Kim *et al.*, "Reducing the metabolic rate of walking and running with a versatile, portable exosuit," *Science*, vol. 365, no. 6454, pp. 668–672, 2019.

[12] B. Lim *et al.*, "Delayed output feedback control for gait assistance with a robotic hip exoskeleton," *IEEE Trans. Robot.*, vol. 35, no. 4, pp. 1055–1062, Aug. 2019.

[13] K. Seo *et al.*, "Adaptive oscillator-based control for active lower-limb exoskeleton and its metabolic impact," in *Proc. IEEE Int. Conf. Robot. Autom. (ICRA)*, 2018, pp. 6752–6758.

[14] A. J. Young, J. Foss, H. Gannon, and D. P. Ferris, "Influence of power delivery timing on the energetics and biomechanics of humans wearing a hip exoskeleton," *Front. Bioeng. Biotechnol.*, vol. 5, p. 4, Mar. 2017.

[15] I. Kang, H. Hsu, and A. Young, "The effect of hip assistance levels on human energetic cost using robotic hip exoskeletons," *IEEE Robot. Autom. Lett.*, vol. 4, no. 2, pp. 430–437, Apr. 2019.

[16] C. L. Lewis and D. P. Ferris, "Invariant hip moment pattern while walking with a robotic hip exoskeleton," *J. Biomech.*, vol. 44, no. 5, pp. 789–793, 2011.

[17] P. Malcolm, W. Derave, S. Galle, and D. De Clercq, "A simple exoskeleton that assists plantar flexion can reduce the metabolic cost of human walking," *PLoS ONE*, vol. 8, no. 2, 2013, Art. no. e56137.

[18] S. Wang *et al.*, "Design and control of the MINDWALKER exoskeleton," *IEEE Trans. Neural Syst. Rehabil. Eng.*, vol. 23, no. 2, pp. 277–286, Mar. 2015.

[19] C. J. Walsh, K. Pasch, and H. Herr, "An autonomous, underactuated exoskeleton for load-carrying augmentation," in *Proc. IEEE/RSJ Int. Conf. Intell. Robots Syst.*, 2006, pp. 1410–1415.

[20] S. A. Murray, K. H. Ha, C. Hartigan, and M. Goldfarb, "An assistive control approach for a lower-limb exoskeleton to facilitate recovery of walking following stroke," *IEEE Trans. Neural Syst. Rehabil. Eng.*, vol. 23, no. 3, pp. 441–449, May 2015.

[21] D. J. Villarreal, D. Quintero, and R. D. Gregg, "Piecewise and unified phase variables in the control of a powered prosthetic leg," in *Proc. IEEE Int. Conf. Rehabil. Robot. (ICORR)*, 2017, pp. 1425–1430.

[22] D. Quintero, D. J. Lambert, D. J. Villarreal, and R. D. Gregg, "Real-time continuous gait phase and speed estimation from a single sensor," in *Proc. IEEE Conf. Control Technol. Appl. (CCTA)*, 2017, pp. 847–852.

[23] R. Ronsse *et al.*, "Oscillator-based assistance of cyclical movements: Model-based and model-free approaches," *Med. Biol. Eng. Comput.*, vol. 49, no. 10, p. 1173, 2011.

[24] F. Giovacchini *et al.*, "A light-weight active orthosis for hip movement assistance," *Robot. Auton. Syst.*, vol. 73, pp. 123–134, Nov. 2015.

[25] K. Seo *et al.*, "RNN-based on-line continuous gait phase estimation from shank-mounted IMUs to control ankle exoskeletons," in *Proc. IEEE 16th Int. Conf. Rehabil. Robot. (ICORR)*, 2019, pp. 809–815.

[26] J. Yang *et al.*, "Machine learning based adaptive gait phase estimation using inertial measurement sensors," in *Proc. Design Med. Devices Conf.*, 2019, Art. no. V001T09A010.

[27] A. Young, T. Kuiken, and L. Hargrove, "Analysis of using EMG and mechanical sensors to enhance intent recognition in powered lower limb prostheses," *J. Neural Eng.*, vol. 11, no. 5, 2014, Art. no. 056021.

[28] I. Kang, P. Kunapuli, H. Hsu, and A. J. Young, "Electromyography (EMG) signal contributions in speed and slope estimation using robotic exoskeletons," in *Proc. IEEE 16th Int. Conf. Rehabil. Robot. (ICORR)*, 2019, pp. 548–553.

[29] Y. LeCun, Y. Bengio, and G. Hinton, "Deep learning," *Nature*, vol. 521, no. 7553, p. 436, 2015.

[30] J. Schmidhuber, "Deep learning in neural networks: An overview," *Neural Netw.*, vol. 61, pp. 85–117, Jan. 2015.

[31] A. J. Young and L. J. Hargrove, "A classification method for user-independent intent recognition for transfemoral amputees using powered lower limb prostheses," *IEEE Trans. Neural Syst. Rehabil. Eng.*, vol. 24, no. 2, pp. 217–225, Feb. 2015.

[32] I. Kang, H. Hsu, and A. J. Young, "Design and validation of a torque controllable hip exoskeleton for walking assistance," in *Proc. ASME Dyn. Syst. Control Conf.*, 2018, Art. no. V001T12A002.

[33] D. A. Winter, "Kinematic and kinetic patterns in human gait: Variability and compensating effects," *Human Movement Sci.*, vol. 3, nos. 1–2, pp. 51–76, 1984.

[34] H. A. Varol, F. Sup, and M. Goldfarb, "Multiclass real-time intent recognition of a powered lower limb prosthesis," *IEEE Trans. Biomed. Eng.*, vol. 57, no. 3, pp. 542–551, Mar. 2010.

[35] R. Bellman, "Dynamic programming," *Science*, vol. 153, no. 3731, pp. 34–37, 1966.

[36] F. Chollet. (2015). *Keras.* [Online]. Available: https://github.com/keras-team/keras

[37] M. Abadi *et al.*, "TensorFlow: A system for large-scale machine learning," in *Proc. 12th USENIX Symp. Oper. Syst. Design Implement. (OSDI)*, 2016, pp. 265–283.

[38] V. K. Ojha, A. Abraham, and V. Snášel, "Metaheuristic design of feedforward neural networks: A review of two decades of research," *Eng. Appl. Artif. Intell.*, vol. 60, pp. 97–116, Apr. 2017.

[39] D. P. Kingma and J. Ba, "Adam: A method for stochastic optimization," in *Proc. Int. Conf. Learn. Represent. (ICLR)*, San Diego, CA, USA, May 2015.

[40] I. Sutskever, J. Martens, G. E. Dahl, and G. E. Hinton, "On the importance of initialization and momentum in deep learning," in *Proc. Int. Conf. Mach. Learn.*, 2013, pp. 1139–1147.

[41] L. Prechelt, "Early stopping-but when?" in *Neural Networks: Tricks of the Trade*. Heidelberg, Germany: Springer, 1998, pp. 55–69.

[42] Y. Ding, M. Kim, S. Kuindersma, and C. J. Walsh, "Human-in-the-loop optimization of hip assistance with a soft exosuit during walking," *Sci. Robot.*, vol. 3, no. 15, 2018, Art. no. eaar5438.

[43] Y. Ding *et al.*, "Effect of timing of hip extension assistance during loaded walking with a soft exosuit," *J. Neuroeng. Rehabil.*, vol. 13, no. 1, p. 87, 2016.

[44] L. Torrey and J. Shavlik, "Transfer learning," in *Handbook of Research on Machine Learning Applications and Trends: Algorithms, Methods, and Techniques*. New York, NY, USA: IGI Glob., 2010, pp. 242–264.

[45] Y. Ding, I. Galiana, C. Siviy, F. A. Panizzolo, and C. J. Walsh, "IMU-based iterative control for hip extension assistance with a soft exosuit," in *Proc. IEEE Int. Conf. Robot. Autom. (ICRA)*, 2016, pp. 3501–3508.

[46] T. G. Sugar *et al.*, "Limit cycles to enhance human performance based on phase oscillators," *J. Mech. Robot.*, vol. 7, no. 1, 2015, Art. no. 011001.

[47] T. Yan, A. Parri, V. R. Garate, M. Cempini, R. Ronsse, and N. Vitiello, "An oscillator-based smooth real-time estimate of gait phase for wearable robotics," *Auton. Robots*, vol. 41, no. 3, pp. 759–774, 2017.

[48] K. Seo, S. Hyung, B. K. Choi, Y. Lee, and Y. Shim, "A new adaptive frequency oscillator for gait assistance," in *Proc. IEEE Int. Conf. Robot. Autom. (ICRA)*, 2015, pp. 5565–5571.

[49] E. Zheng, S. Manca, T. Yan, A. Parri, N. Vitiello, and Q. Wang, "Gait phase estimation based on noncontact capacitive sensing and adaptive oscillators," *IEEE Trans. Biomed. Eng.*, vol. 64, no. 10, pp. 2419–2430, Oct. 2017.

[50] S. Crea *et al.*, "Controlling a robotic hip exoskeleton with noncontact capacitive sensors," *IEEE/ASME Trans. Mechatronics*, vol. 24, no. 5, pp. 2227–2235, Oct. 2019.

[51] B. W. Stansfield, S. J. Hillman, M. E. Hazlewood, and J. E. Robb, "Regression analysis of gait parameters with speed in normal children walking at self-selected speeds," *Gait Posture*, vol. 23, no. 3, pp. 288–294, 2006.

[52] K. Kosanovich, A. Gurumoorthy, E. Sinzinger, and M. Piovoso, "Improving the extrapolation capability of neural networks," in *Proc. IEEE Int. Symp. Intell. Control*, 1996, pp. 390–395.

[53] R. A. Mann and J. Hagy, "Biomechanics of walking, running, and sprinting," *Amer. J. Sports Med.*, vol. 8, no. 5, pp. 345–350, 1980.

[54] S. H. Collins, M. B. Wiggin, and G. S. Sawicki, "Reducing the energy cost of human walking using an unpowered exoskeleton," *Nature*, vol. 522, no. 7555, pp. 212–215, 2015.

[55] S. J. Pan and Q. Yang, "A survey on transfer learning," *IEEE Trans. Knowl. Data Eng.*, vol. 22, no. 10, pp. 1345–1359, Oct. 2010.